LETTERS

Microtubule nucleating γ-TuSC assembles structures with 13-fold microtubule-like symmetry

Justin M. Kollman[1], Jessica K. Polka[2], Alex Zelter[3], Trisha N. Davis[3] & David A. Agard[1]

Microtubules are nucleated *in vivo* by γ-tubulin complexes. The 300-kDa γ-tubulin small complex (γ-TuSC), consisting of two molecules of γ-tubulin and one copy each of the accessory proteins Spc97 and Spc98, is the conserved, essential core of the microtubule nucleating machinery[1,2]. In metazoa multiple γ-TuSCs assemble with other proteins into γ-tubulin ring complexes (γ-TuRCs). The structure of γ-TuRC indicated that it functions as a microtubule template[2–5]. Because each γ-TuSC contains two molecules of γ-tubulin, it was assumed that the γ-TuRC-specific proteins are required to organize γ-TuSCs to match 13-fold microtubule symmetry. Here we show that *Saccharomyces cerevisiae* γ-TuSC forms rings even in the absence of other γ-TuRC components. The yeast adaptor protein Spc110 stabilizes the rings into extended filaments and is required for oligomer formation under physiological buffer conditions. The 8-Å cryo-electron microscopic reconstruction of the filament reveals 13 γ-tubulins per turn, matching microtubule symmetry, with plus ends exposed for interaction with microtubules, implying that one turn of the filament constitutes a microtubule template. The domain structures of Spc97 and Spc98 suggest functions for conserved sequence motifs, with implications for the γ-TuRC-specific proteins. The γ-TuSC filaments nucleate microtubules at a low level, and the structure provides a strong hypothesis for how nucleation is regulated, converting this less active form to a potent nucleator.

Microtubules assembled *in vitro* have a broad distribution of protofilament numbers centred on 14 (ref. 6). However, microtubules nucleated in cells mostly have 13 protofilaments[7], suggesting that γ-tubulin complexes constrain microtubule geometry. Thirteen-fold symmetry is probably preferred because it allows the protofilaments to run straight along the microtubule (as opposed to being twisted in other protofilament symmetries), allowing motor proteins tracking processively to remain on one face of the microtubule. It has generally been assumed that γ-TuRC-specific proteins form a cap-like structure that establishes 13-fold symmetry by providing a scaffold for γ-TuSC assembly. How γ-TuSC is organized in organisms such as *Saccharomyces cerevisiae*, which lack all of the γ-TuRC-specific proteins, has remained an open question.

The sequence and structural similarity between γ-tubulin and α/β-tubulin indicated that nucleation results from microtubule-like contacts between γ-tubulin and α/β-tubulin[8]. The microtubule lattice consists of lateral and longitudinal contacts[9,10]; the stronger longitudinal contacts define microtubule polarity, with plus and minus ends (Supplementary Fig. 1). The template model for microtubule nucleation predicts that γ-tubulins interact laterally to form a ring that makes longitudinal contacts with α/β-tubulin[2–5] minus ends; alternative models that predict lateral interactions between γ-tubulin and α/β-tubulin[11] have not been definitively ruled out.

Our previous 25-Å structure of *Saccharomyces* γ-TuSC was determined in buffer conditions that yielded predominantly monomeric complexes[12,13]. Here we show that buffer conditions that promote microtubule growth (BRB80: low salt, pH 6.9) also promote the spontaneous assembly of γ-TuSCs into rings similar to *Drosophila* γ-TuRCs[2,4] (Fig. 1a, b). Ring formation was sensitive to both salt and pH (Supplementary Fig. 2a–c). The γ-TuSC rings bound microtubules, and many of these microtubule ends are capped (Fig. 1c), in a similar manner to microtubules nucleated *in vivo*[14,15] or from γ-TuRCs *in vitro*[3,4,16]. Spontaneous assembly suggests that ring formation is an intrinsic property of γ-TuSC, and is not dependent on γ-TuRC-specific proteins.

The amino-terminal 220 residues of Spc110 (Spc110$^{1–220}$), which attaches γ-TuSC to the nuclear face of the yeast spindle pole body, markedly increased the stability and length of γ-TuSC assemblies (Fig. 1d). Co-purification with Spc110$^{1–220}$ yielded a continuum of γ-TuSC oligomers ranging from dimers to long, well-ordered helical filaments, even under conditions where γ-TuSC alone fails to assemble (Supplementary Fig. 2d–f). We determined the three-dimensional structure of γ-TuSC filaments from cryo-electron micrographs (Fig. 2a), using iterative helical real-space reconstruction, a single-particle approach to helical structure determination[17]. The resolution of the reconstruction, which included about 25,000 γ-TuSC subunits, was estimated at 8 Å by the Fourier shell correlation 0.5 cutoff (Fig. 2b).

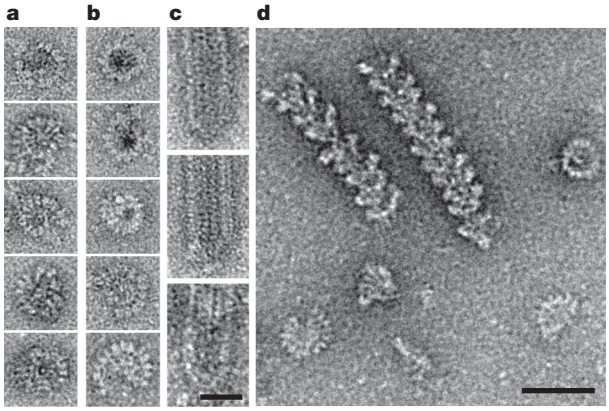

Figure 1 | γ-TuSC oligomers form spontaneously and are stabilized by Spc110. a, Ring-like structures were observed in negative-stain electron micrographs of *Saccharomyces* γ-TuSC at pH 6.9. **b**, γ-TuRC purified from *Drosophila* embryos is similar in shape and size to the γ-TuSC rings. **c**, Capped ends were observed on microtubules grown in the presence of preformed γ-TuSC rings. **d**, Negative-stain images of γ-TuSC filaments formed on co-purification with Spc110$^{1–220}$. Scale bars, 25 nm (**a**–**c**) and 50 nm (**d**).

[1]Department of Biochemistry and Biophysics, Howard Hughes Medical Institute, and Keck Advanced Microscopy Center, University of California, San Francisco, San Francisco, California 94158, USA. [2]Cellular and Molecular Pharmacology, University of California, San Francisco, San Francisco, California 94158, USA. [3]Department of Biochemistry, University of Washington, Seattle, Washington 98195, USA.

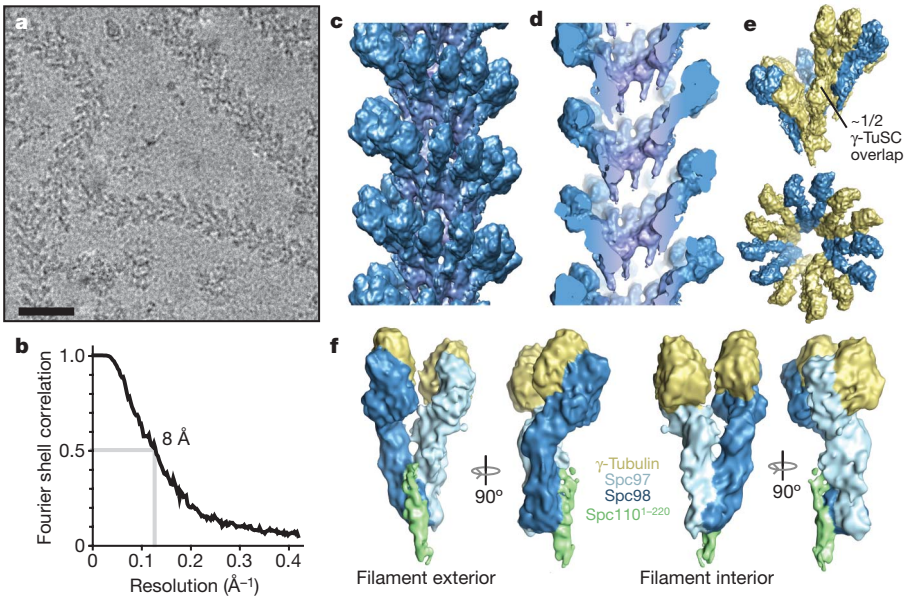

Figure 2 | γ-TuSC filament structure. **a**, Cryo-electron micrograph of γ-TuSC filaments. Scale bar, 50 nm. **b**, The resolution of the structure is estimated to be 8 Å by the Fourier shell correlation. **c**, A segment of the reconstructed filament filtered to 8 Å. **d**, A cutaway view of the filament, illustrating the lack of connection between helical layers. **e**, One turn of the helix, coloured by γ-TuSC. The filament has 6½ γ-TuSCs per turn, with a half γ-TuSC overlap. **f**, A single γ-TuSC/Spc110$^{1–220}$ subunit from the filament, with the approximate boundaries between the individual proteins indicated by colour.

The filament is a single spiral of laterally associated γ-TuSCs, without contact between layers (Fig. 2c, d and Supplementary Movie 1). The helical symmetry (54.3° rotation and 22.2 Å rise per subunit) gives rise to just over 6½ γ-TuSCs—or 13 γ-tubulins—per turn, with a half γ-TuSC overlap. Each turn of helix forms a lock-washer shape similar to that of γ-TuRC[4] (Fig. 2e). The 13-fold γ-tubulin symmetry of the filament is dictated largely by the extensive lateral interactions between Spc97 and Spc98 of adjacent γ-TuSCs (Fig. 2e and Supplementary Fig. 6a), locking in the lateral tubulin contacts, which on their own are flexible enough to accommodate a range of different symmetries. We propose that a γ-TuSC assembly very similar to a single ring from the filament provides the constraint that limits microtubules to 13 protofilaments in all eukaryotes *in vivo*[7].

γ-TuSC in the filament is remarkably similar to free γ-TuSC[13,18] (Fig. 2f and Supplementary Fig. 3), indicating that oligomerization does not induce large-scale conformational changes. The 8-Å structure provides new insight into the domain architecture of Spc97 and Spc98: they dimerize at their N-terminal ends nearest the helical axis, and have extended central domains connecting to carboxy-terminal γ-tubulin-binding domains. The central domain of Spc98 is kinked, at a position previously shown to be the site of limited hinge-like flexibility[13]. The masses of the domains determined from the cryo-electron microscopy map provide a rough estimate of their boundaries in each sequence, indicating the positions of the grip1 and grip2 motifs, conserved in all γ-tubulin complex proteins[19] (Supplementary Fig. 4a, b). The grip2 motif covers nearly half of the C-terminal domains, strongly suggesting that it is important for γ-tubulin binding. The grip1 motif is in the central domain, near inter-γ-TuSC contacts and the kink in Spc98. We tentatively assign Spc110$^{1–220}$ to a ridge of density running along the exterior face of γ-TuSC in the filament, making contacts primarily with Spc98 (Supplementary Fig. 3). The resolution of the reconstruction seems to be non-uniform, as tubes of α-helical density are clear in the N-terminal domains of Spc97 and Spc98 at the core of the structure, but secondary structure features are not well defined in the peripheral density, where γ-tubulin is located (Supplementary Fig. 5). The lower effective resolution in the γ-tubulin regions may be due to limited flexibility in the weak connections between the central and C-terminal domains of Spc97 and Spc98.

The human γ-tubulin crystal structure[20] was fitted into the density in the regions previously assigned to γ-tubulin[13] (Fig. 3a, b). The minus-end longitudinal surface of γ-tubulin is completely buried in the interface with Spc97/Spc98. The lateral contacts between γ-tubulins of

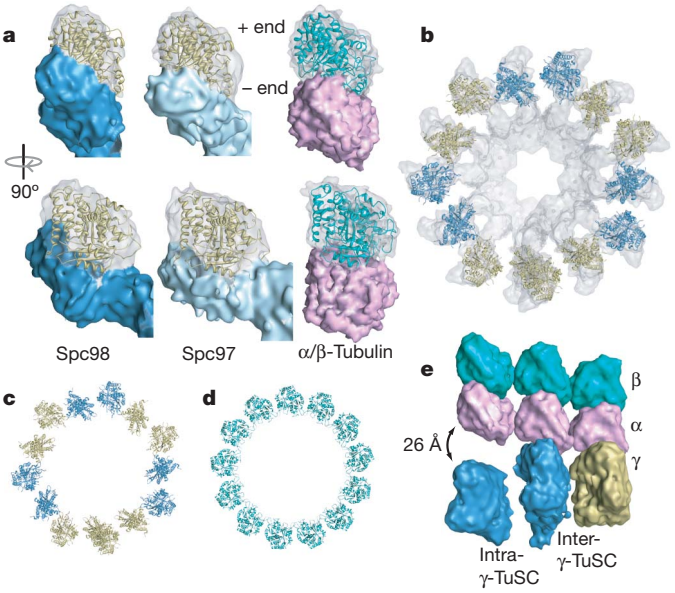

Figure 3 | γ-Tubulin in the γ-TuSC filament has a geometry similar to 13-protofilament microtubules. **a**, The electron microscopic densities of γ-tubulin (transparent) and the Spc97/Spc98-binding domains (opaque) are shown with the γ-tubulin crystal structure fitted in the density. The density is tilted relative to the helical axis so that in each case the plus end is vertical. An α/β-tubulin heterodimer is shown with simulated electron microscopic density for comparison. **b**, Thirteen γ-tubulins fit into one turn of the filament. Neighbouring γ-tubulins in the same γ-TuSC are the same colour. **c**, **d**, The γ-tubulin symmetry (**c**) is similar to that of a 13-protofilament microtubule (**d**), but separated intra-γ-TuSC γ-tubulins alternate with contacting inter-γ-TuSC γ-tubulins. **e**, To illustrate the mismatch between geometries, laterally interacting α/β-tubulin heterodimers were aligned to the filament so that the central α/β-tubulin makes longitudinal contacts to γ-tubulin.

neighbouring γ-TuSCs are nearly identical to microtubule lateral contacts. The two γ-tubulins within each γ-TuSC are skewed slightly apart, in a configuration incompatible with the microtubule lattice (Fig. 3b, c), as observed in the free γ-TuSC structure[13]. This symmetry gives rise to an alternating pattern of γ-tubulin pairs with microtubule-like lateral spacing separated by gaps, generating a staggered mismatch with the microtubule lattice (Fig. 3c–e). The only microtubule lattice surface of γ-tubulin fully exposed in the filament is the plus-end face, favouring a model in which γ-tubulin makes longitudinal contacts with α/β-tubulin. This, combined with the 13-fold γ-tubulin symmetry, provides the strongest evidence so far to support a γ-tubulin template mechanism for microtubule nucleation.

We tested the capacity of γ-TuSC oligomers to nucleate microtubules (Fig. 4). At pH 6.9 both γ-TuSC alone and γ-TuSC filaments provided modest levels of nucleation, slightly higher for γ-TuSC filaments than for γ-TuSC alone. At pH 7.5 γ-TuSC alone does not nucleate microtubules, whereas the filaments retain a low level of nucleation. As γ-TuSC rings do not form at pH 7.5, but γ-TuSC filaments remain intact (Supplementary Fig. 2b, c), these results suggest that γ-TuSC nucleation activity is assembly-dependent. The levels of nucleation observed are consistent with previous measurements for γ-TuSC[2,21] but are less robust than seen with γ-TuRC[2,5], suggesting that assembly alone is insufficient to fully activate γ-TuSC nucleating activity. The arrangement of γ-tubulin in γ-TuSC oligomers provides a structural explanation for their relatively modest nucleating activity. Nucleation probably arises from the inter-γ-TuSC γ-tubulin pairs, which have the correct microtubule lattice spacing. Simulations indicate that a γ-TuSC assembly in which all of the γ-tubulins make lateral microtubule-like contacts would provide greatly enhanced nucleation (L. Rice, personal communication).

The structure provides a clear hypothesis for how nucleation could be fully activated. We previously predicted that bending at the flexible kink in Spc98 is required to bring the intra-γ-TuSC γ-tubulins to the microtubule spacing[13,18]. We speculated that γ-TuSC assembly might drive this change, but that clearly is not so—a similar conformational change is still required in γ-TuSC rings. In the lower-resolution γ-TuSC structure we predicted that the movement would be a closure of the gap between γ-tubulins; here we see that the movement must be more perpendicular to the edge of the ring, bringing γ-tubulin in towards the helical axis. A rotation of 23° about the kink in Spc98 would reposition γ-tubulin by 26 Å, bringing it to the microtubule lattice spacing (Supplementary Fig. 7 and Supplementary Movies 2 and 3). The staggered γ-tubulin arrangement probably serves a regulatory function, maintaining γ-TuSC oligomers in a low-activity state until a signal (such as protein binding or post-translational modification) directs the rearrangements in Spc98 necessary to form a template with exact microtubule lattice geometry. Although less likely, rearrangement of the γ-tubulins could be induced by binding of α/β-tubulin. In such a model γ-TuSC would function primarily as a cap for stabilizing and localizing microtubule minus ends, rather than as a strong nucleator.

The marked enhancement of γ-TuSC oligomer stability by Spc110, combined with its role in γ-TuSC localization, probably serves to ensure that microtubule template assembly in yeast occurs only at the spindle pole body. We propose a general model for microtubule nucleation in which Spc110 or its functional equivalent directly attaches γ-TuSC to microtubule organizing centres, promoting template assembly. A subsequent activation step then fully activates nucleation by rearranging the γ-tubulin network (Fig. 5a). In a template with seven γ-TuSCs, the location of the half γ-TuSC overlap defines the position of the 13-protofilament microtubule seam; a single lateral contact between γ-tubulin and α-tubulin would be made at the overlap, as well. It is unclear how many γ-TuSCs are required to nucleate a microtubule—an incomplete ring may be sufficient to initiate growth.

The γ-TuSC filament structure provides unique insight into the roles of γ-TuRC-specific proteins. Our results clearly show that γ-TuSC assembly alone establishes 13-fold γ-tubulin symmetry, indicating that the γ-TuRC-specific proteins are not required as a scaffold. This is consistent with the observation that all of the γ-TuRC-specific proteins can be depleted without affecting centrosomal microtubule nucleation of 13-protofilament microtubules[22,23]. Although not required as a scaffold, the γ-TuRC-specific proteins may serve to stabilize the ring structure or fully activate nucleation activity, and they are essential for γ-TuRC localization at non-centrosomal sites, as in augmin-dependent binding within the mitotic spindle[24] (Fig. 5b).

We suggested earlier that the grip1 and grip2 motifs, conserved in all the γ-TuRC-specific proteins, are involved in ring assembly contacts and γ-tubulin binding, respectively. This raises the possibility that the γ-TuRC-specific proteins may each bind γ-tubulin and

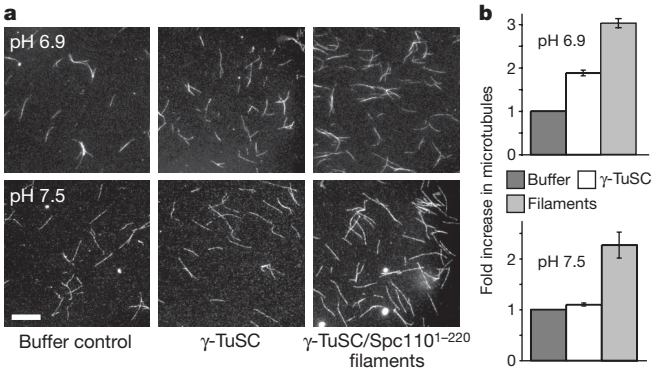

Figure 4 | γ-TuSC oligomers nucleate microtubules at low levels. **a**, Fluorescence micrographs of rhodamine-labelled microtubules assembled at pH 6.9 or 7.5 in the presence of buffer, γ-TuSC or γ-TuSC/Spc110$^{1–220}$ filaments (final γ-TuSC concentration 150 nM). Scale bar, 5 μm. **b**, The mean number of microtubules per field is shown for nucleation at pH 6.9 ($n = 5$) and pH 7.5 ($n = 3$). Error bars represent s.e.m.

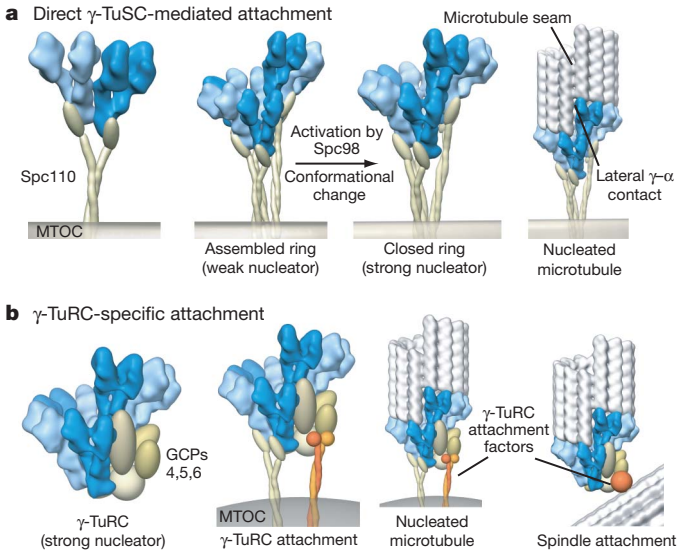

Figure 5 | Models of nucleation complex attachment and activation. **a**, In the absence of γ-TuRC-specific components, as in *Saccharomyces*, Spc110 or its equivalent directly attaches γ-TuSC to microtubule-organizing centres (MTOCs), promoting ring assembly. We propose that a conformational change in Spc98 promotes nucleation by rearranging γ-tubulin into an exact microtubule template. **b**, In organisms with complete γ-TuRCs, active complexes attach to organizing centres directly through γ-TuSCs, or potentially through unique sites in the γ-TuRC-specific components. Localization of γ-TuRCs at non-MTOC locations, for example within the mitotic spindle, is mediated through the γ-TuRC-specific proteins. In both models, γ-TuSC interactions define the geometry of the nucleating template.

substitute for Spc97 or Spc98 in the ring itself. To do this, they might form hybrid γ-TuSCs with one of the γ-TuRC-specific proteins plus Spc97 or Spc98, alternative γ-TuSCs with two different γ-TuRC-specific proteins, or unique half γ-TuSCs (Supplementary Fig. 8). Such alternative γ-TuSCs might serve to initiate or terminate γ-TuSC oligomerization, or to stabilize the ring at the overlapping ends, while providing unique attachment sites in the structure of the ring itself.

METHODS SUMMARY

γ-TuSC was co-expressed with glutathione *S*-transferase (GST)–Spc110$^{1–220}$ as described[13,21], except that complexes were eluted by cleavage of the GST tag with tobacco etch virus (TEV) protease as the final purification step. γ-TuSC rings were formed by incubation for 30 min on ice after dilution to 0.2 μM in BRB80 (80 mM PIPES pH 6.9, 1 mM EGTA, 1 mM $MgCl_2$). Nucleation assays were performed essentially as described[21]. The cryo-electron microscopic reconstruction was performed essentially as described[17,25].

Full Methods and any associated references are available in the online version of the paper at www.nature.com/nature.

Received 19 April; accepted 27 May 2010.
Published online 14 July 2010.

1. Knop, M. & Schiebel, E. Spc98p and Spc97p of the yeast γ-tubulin complex mediate binding to the spindle pole body via their interaction with Spc110p. *EMBO J.* **16,** 6985–6995 (1997).
2. Oegema, K. *et al.* Characterization of two related *Drosophila* γ-tubulin complexes that differ in their ability to nucleate microtubules. *J. Cell Biol.* **144,** 721–733 (1999).
3. Keating, T. J. & Borisy, G. G. Immunostructural evidence for the template mechanism of microtubule nucleation. *Nature Cell Biol.* **2,** 352–357 (2000).
4. Moritz, M., Braunfeld, M. B., Guenebaut, V., Heuser, J. & Agard, D. A. Structure of the γ-tubulin ring complex: a template for microtubule nucleation. *Nature Cell Biol.* **2,** 365–370 (2000).
5. Zheng, Y., Wong, M. L., Alberts, B. & Mitchison, T. Nucleation of microtubule assembly by a γ-tubulin-containing ring complex. *Nature* **378,** 578–583 (1995).
6. Chretien, D. & Wade, R. H. New data on the microtubule surface lattice. *Biol. Cell* **71,** 161–174 (1991).
7. Evans, L., Mitchison, T. & Kirschner, M. Influence of the centrosome on the structure of nucleated microtubules. *J. Cell Biol.* **100,** 1185–1191 (1985).
8. Oakley, B. R., Oakley, C. E., Yoon, Y. & Jung, M. K. γ-Tubulin is a component of the spindle pole body that is essential for microtubule function in Aspergillus nidulans. *Cell* **61,** 1289–1301 (1990).
9. Nogales, E., Wolf, S. G. & Downing, K. H. Structure of the αβ tubulin dimer by electron crystallography. *Nature* **391,** 199–203 (1998).
10. Nogales, E., Whittaker, M., Milligan, R. A. & Downing, K. H. High-resolution model of the microtubule. *Cell* **96,** 79–88 (1999).
11. Erickson, H. P. γ-Tubulin nucleation: template or protofilament? *Nature Cell Biol.* **2,** E93–E96 (2000).
12. Aldaz, H., Rice, L. M., Stearns, T. & Agard, D. A. Insights into microtubule nucleation from the crystal structure of human γ-tubulin. *Nature* **435,** 523–527 (2005).
13. Kollman, J. M. *et al.* The structure of the γ-tubulin small complex: implications of its architecture and flexibility for microtubule nucleation. *Mol. Biol. Cell* **19,** 207–215 (2008).
14. Byers, B., Shriver, K. & Goetsch, L. The role of spindle pole bodies and modified microtubule ends in the initiation of microtubule assembly in *Saccharomyces cerevisiae*. *J. Cell Sci.* **30,** 331–352 (1978).
15. Moritz, M. *et al.* Three-dimensional structural characterization of centrosomes from early *Drosophila* embryos. *J. Cell Biol.* **130,** 1149–1159 (1995).
16. Wiese, C. & Zheng, Y. A new function for the γ-tubulin ring complex as a microtubule minus-end cap. *Nature Cell Biol.* **2,** 358–364 (2000).
17. Egelman, E. H. A robust algorithm for the reconstruction of helical filaments using single-particle methods. *Ultramicroscopy* **85,** 225–234 (2000).
18. Choy, R. M., Kollman, J. M., Zelter, A., Davis, T. N. & Agard, D. A. Localization and orientation of the γ-tubulin small complex components using protein tags as labels for single particle EM. *J. Struct. Biol.* **168,** 571–574 (2009).
19. Gunawardane, R. N. *et al.* Characterization and reconstitution of *Drosophila* γ-tubulin ring complex subunits. *J. Cell Biol.* **151,** 1513–1524 (2000).
20. Rice, L. M., Montabana, E. A. & Agard, D. A. The lattice as allosteric effector: structural studies of αβ- and γ-tubulin clarify the role of GTP in microtubule assembly. *Proc. Natl Acad. Sci. USA* **105,** 5378–5383 (2008).
21. Vinh, D. B., Kern, J. W., Hancock, W. O., Howard, J. & Davis, T. N. Reconstitution and characterization of budding yeast γ-tubulin complex. *Mol. Biol. Cell* **13,** 1144–1157 (2002).
22. Goshima, G. *et al.* Genes required for mitotic spindle assembly in *Drosophila* S2 cells. *Science* **316,** 417–421 (2007).
23. Verollet, C. *et al. Drosophila melanogaster* γ-TuRC is dispensable for targeting γ-tubulin to the centrosome and microtubule nucleation. *J. Cell Biol.* **172,** 517–528 (2006).
24. Goshima, G., Mayer, M., Zhang, N., Stuurman, N. & Vale, R. D. Augmin: a protein complex required for centrosome-independent microtubule generation within the spindle. *J. Cell Biol.* **181,** 421–429 (2008).
25. Sachse, C. *et al.* High-resolution electron microscopy of helical specimens: a fresh look at tobacco mosaic virus. *J. Mol. Biol.* **371,** 812–835 (2007).

Supplementary Information is linked to the online version of the paper at www.nature.com/nature.

Acknowledgements We thank M. Braunfeld and A. Avila-Sakar for microscopy assistance; Y. Cheng, E. Muller, M. Moritz and K. Huang for helpful discussions; and B. Carragher, C. Potter and J. Quispe for the use of their electron microscopy facilities and technical assistance with data collection. Some of the work presented here was conducted at the National Resource for Automated Molecular Microscopy, which is supported by the National Institutes of Health (NIH) through the National Center for Research Resources' P41 program. This work was supported by the NIH (D.A.A. and T.N.D.) and the Howard Hughes Medical Institute (D.A.A.). J.M.K. was a NIH Ruth L. Kirschstein National Research Service Award (NRSA) postdoctoral fellow.

Author Contributions J.M.K. purified and prepared samples for electron microscopy, collected cryo-electron microscopy data, determined the structure and performed microtubule nucleation experiments. J.K.P. explored γ-TuSC assembly conditions and prepared and imaged capped microtubules. A.Z. designed and cloned expression constructs, and generated and tested baculovirus strains. D.A.A and J.M.K. designed experiments and analysed data. J.M.K., D.A.A. and T.N.D. wrote the paper. All the authors discussed the results and commented on the manuscript.

Author Information The cryo-electron microscopic reconstruction is deposited with the Electron Microscopy Database with the accession code 1731. Reprints and permissions information is available at www.nature.com/reprints. The authors declare no competing financial interests. Readers are welcome to comment on the online version of this article at www.nature.com/nature. Correspondence and requests for materials should be addressed to D.A.A. (agard@msg.ucsf.edu).

METHODS

Sample preparation. γ-TuSC was co-expressed with GST–Spc110$^{1-220}$ in Sf9 cells and purified as described, in H100 buffer (40 mM Hepes pH 7.6, 100 mM KCl, 1 mM EGTA, 1 mM $MgCl_2$)[13,21], except that complexes were eluted from glutathione resin by cleavage of the GST tag with TEV protease as the final purification step. γ-TuSC rings were formed by a 30-min incubation on ice after dilution to 0.2 μM in BRB80 (80 mM PIPES pH 6.9, 1 mM EGTA, 1 mM $MgCl_2$). For cryo-electron microscopy, γ-TuSC/Spc110$^{1-220}$ filaments were at 2 mg ml^{-1} total protein in H100. γ-TuRCs were purified from *Drosophila* embryos as described[2]. Microtubules were grown in the presence of γ-TuSC rings and prepared for electron microscopy as described[3], with the exception that microtubules were crosslinked for 3 min in 1% glutaraldehyde before sedimentation. Negative-stain samples were prepared as described[26] in 0.75% uranyl formate, and cryo-electron microscopy samples were prepared on C-FLAT holey carbon grids[27] with a Vitrobot (FEI Co.).

Electron microscopy and image processing. Negative-stain electron microscopy was performed on a Tecnai T12 Spirit (FEI Co.) operating at 120 kV, and images were acquired on a 4k × 4k charge-coupled device camera (Gatan, Inc.). Cryo-electron microscopy data were obtained on a Tecnai F20 operating at 200 kV with an 8k × 8k TemCam-F816 camera (TVIPS) with a pixel size of 1.19 Å per pixel. Defocus was determined with CTFFIND[28], and each micrograph was corrected by application of a Wiener filter. Particles were boxed out in 505-Å segments, overlapping by 480 Å. After several initial rounds of alignment, the particles were centred with respect to the helix axis by integer pixel shifts, then masked to 310 Å along the helical axis and 380 Å perpendicular to the axis with a cosine-edged mask.

Iterative helical real-space reconstruction was performed essentially as described[17,25], using SPIDER[29]. Initially, 18 rounds of projection matching were performed with 2× binned particles, with the helical symmetry parameters refined and imposed at each step with the programs hsearch_lorentz and himpose[17]. In subsequent rounds, helical symmetry parameters were fixed, real-space symmetry was imposed with SPIDER, and refinement was limited to searching within 2° of orientation assignments from the previous round. Seven rounds of refinement were performed, after which particles were re-masked to 160 Å along the helical axis (corresponding to about 1.3 turns of helix) to reduce the effects of bending in the helix. Five rounds of refinement were performed with these masked particles, then a final 15 rounds using the unbinned, masked particles.

A 300-Å^2 *B*-factor was applied to the final reconstruction by using the program BFACTOR. Volumes were viewed and segmented with Chimera[30]. Automated segmentation of Spc97 and Spc98 into domains was performed with the Chimera plug-in Segger. The crystal structure of γ-tubulin was fitted into the density by initial manual placement and then fitting with the Chimera fitting routine.

Microtubule nucleation assays. The solution nucleation assays were performed essentially as described[21]. Rhodamine-labelled tubulin in assembly buffer (BRB80; 25% glycerol, 1 mM GTP) was incubated on ice for 5 min with γ-TuSC or γ-TuSC/Spc110$^{1-220}$ filaments (150 nM final γ-TuSC concentration) or H100 as a buffer control. The assembly reactions were transferred to a 37 °C water bath for 4 min, diluted tenfold in warm assembly buffer containing 1% glutaraldehyde to crosslink microtubules for 3 min, then diluted 20-fold in cold BRB80. BRB80 was at pH 6.9 or 7.5, with 1.2 mg ml^{-1} tubulin for the pH 6.9 experiments and 2.0 mg ml^{-1} tubulin for the pH 7.5 experiments.

The crosslinked microtubules were spun through a cushion of BRB80 containing 20% glycerol onto polylysine-coated coverslips. Microtubules were imaged by rhodamine fluorescence on an Axiovert microscope, with images recorded on a charge-coupled device camera. Microtubules were counted in 15 random fields for each experiment, and the values for each experiment were normalized against the buffer control.

26. Ohi, M., Li, Y., Cheng, Y. & Walz, T. Negative staining and image classification—powerful tools in modern electron microscopy. *Biol. Proced. Online* **6,** 23–34 (2004).
27. Quispe, J. *et al.* An improved holey carbon film for cryo-electron microscopy. *Microsc. Microanal.* **13,** 365–371 (2007).
28. Mindell, J. A. & Grigorieff, N. Accurate determination of local defocus and specimen tilt in electron microscopy. *J. Struct. Biol.* **142,** 334–347 (2003).
29. Frank, J. *Three-Dimensional Electron Microscopy of Macromolecular Assemblies* (Academic, 1996).
30. Pettersen, E. F. *et al.* UCSF Chimera—a visualization system for exploratory research and analysis. *J. Comput. Chem.* **25,** 1605–1612 (2004).